# Mechanisms of β-Adrenergic Stimulation of Cardiac $Ca^{2+}$ Channels Revealed by Discrete-Time Markov Analysis of Slow Gating

Stefan Herzig,* Parag Patil,‡ Joachim Neumann,§ Carl-Michael Staschen,¶ and David T. Yue‡

*Department of Pharmacology, University of Kiel, W-2300 Kiel, Germany; §Department of Pharmacology, University of Hamburg, W-2000 Hamburg, Germany; ¶Division of Physiology and Pharmacology, Naval Medical Institute, W-2300 Kronshagen, Germany; ‡Department of Biomedical Engineering, Johns Hopkins University School of Medicine, Baltimore, Maryland 21205 USA

ABSTRACT Individual cardiac $Ca^{2+}$ channels cycle slowly between a mode of gating in which the channel is available to open, and one in which the channel remains silent. The regulation of this multisecond cycling process by isoproterenol was investigated by single-channel recording and the development of a discrete-time Markov model that describes the slow switching among modes in terms of (de)phosphorylation reactions. The results provide evidence that isoproterenol increases $Ca^{2+}$ channel activity by a reciprocal regulatory mechanism: not only is the phosphorylation rate of the channel increased, but also the dephosphorylation rate decreased. The discrete-time Markov formalism should prove useful as a general tool for understanding the mode switching demonstrated by a number of ionic channels.

## INTRODUCTION

A hallmark of β-adrenergic stimulation of individual cardiac L-type $Ca^{2+}$ channels is an increase in the fraction of depolarizing voltage steps that can activate openings (active sweeps), and a decrease in steps without openings (blank sweeps). When depolarizing voltage steps are delivered at regular intervals of about a second, active sweeps cluster together (as do blank sweeps) in a strikingly nonrandom manner (Cavalie et al., 1986), consistent with the proposal that phosphate donation and withdrawal directly underlie sweep clustering (Tsien et al., 1986). The main idea is that of a direct correspondence between a channel being phosphorylated by protein kinase A (PKA) and its availability to open upon depolarization (Kameyama et al., 1986a, 1986b; Ono and Fozzard, 1992). The concept is bolstered by direct biochemical evidence that the main $\alpha_1$ subunit of the cardiac $Ca^{2+}$ channel is in fact phosphorylated in vivo by PKA (Yoshida et al., 1992). Hence, quantitative analysis of sweep clustering offers the attractive possibility of determining the kinetics of phosphorylation of a single molecule in situ.

Problems with this simple proposal began to emerge with the work of Ochi and Kawashima (1990). They certainly demonstrated that β-adrenergic stimulation reduced the mean lifetime of uninterrupted clusters, or runs of blank sweeps, which seems consistent with an enhanced phosphorylation rate by increased PKA activity. The difficulty arises with the observed increase in the average length of runs of active sweeps, which might implicate a decreased dephosphorylation rate according to the simple scheme above. The latter observation conflicts with the commonly accepted β-adrenergic cascade that leads to enhanced PKA activity, without explicit change in phosphatase activity. This discrepancy could arise in several ways:

1) The fundamental assumption of an intimate relation between channel availability and phosphorylation could be in error; the interrelation might be considerably more indirect (Ochi and Kawashima, 1990).

2) There could be a problem with our casual interpretation of the length of runs of active sweeps. Since channel availability is only determined at discrete intervals when voltage steps are delivered, a string of consecutive active sweeps could in fact be punctuated by periods of channel unavailability falling between voltage steps. Hence, an increase in the mean length of active sweep runs need not be correlated in a simple way with decreased dephosphorylation rate. A more precise quantitative method is required to interpret the changes in sweep clustering.

3) Phosphorylation of any one of several sites could render the channel available to open. Then, a higher degree of phosphorylation might extend the length of clusters of active sweeps, because any one of several phosphates could keep the channel available to open.

4) Along with β-adrenergic stimulation, there could be a reduction of channel dephosphorylation rate, since recent biochemical evidence points to activation of an endogenous phosphatase inhibitor in isoproterenol-treated hearts (Ahmad et al., 1989; Neumann et al., 1991).

To distinguish among these possibilities, we developed a general, discrete-time Markov model formalism for analyzing the clustering of active and blank sweeps. Analysis of single-channel data obtained in guinea pig ventricular myocytes exposed to isoproterenol and/or okadaic acid (a selective protein phosphatase inhibitor (Hescheler et al., 1988; Cohen et al., 1990)) supports the latter hypothesis. This report thereby suggests that the dephosphorylation reaction plays an important role in β-adrenergic regulation of cardiac L-type $Ca^{2+}$ channels. Preliminary accounts of this work have been communicated (Herzig and Neumann, 1992; Patil et al., 1993).

*Received for publication 23 February 1993 and in final form 12 July 1993.*

Address correspondence to Dr. Stefan Herzig at Department of Pharmacology, University of Kiel, W-2300 Kiel, Germany, or to Dr. David T. Yue at Department of Biomedical Engineering, Ross Bldg. 713, Johns Hopkins University School of Medicine, 720 Rutland Avenue, Baltimore, MD 21205.



0006-3495/93/10/1599/14 $2.00

## MATERIALS AND METHODS

### Heart cell isolation

Guinea pig ventricular myocytes were enzymatically isolated as described by Mitra and Morad (1985), with slight modifications (below). Hearts were perfused (48 mm Hg, 39°C) in $Ca^{2+}$-free, modified Tyrode's solution (in millimolar: NaCl 135, KCl 4, $NaH_2PO_4$ 0.3, $MgCl_2$ 1, 4-(2-hydroxyethyl)--1-piperazineethanesulfonic acid (HEPES) 10, dextrose 10, pH 7.3) for 5 min. During the next 8–10 min, collagenase (Type 1; Sigma, 1 mg/min) and protease (Type 14; Sigma, 0.7 mg/min) were added. Following this treatment, the hearts were perfused for 5 min with a solution containing (in millimolar) potassium glutamate 120, KCl 25, $MgCl_2$ 2, CaATP 1, EGTA 2, HEPES 10, pH 7.3. Hearts were then minced, and cells dispersed by gentle agitation. Cells were kept in the same solution for storage and recording.

### Electrophysiology

Cell-attached, single-channel recordings were performed as described (Yue et al., 1990b). Pipettes (5–10 MΩ) contained (in millimolar): $BaCl_2$ 70, sucrose 110, HEPES 10, pH 7.4, with TEA-OH. Voltage steps lasting 150 ms (to +20 from −100 mV) were delivered every 0.6 s. Elementary currents were lowpass-filtered at 1 kHz (−3 dB; 4-pole Bessel) and sampled at 10 kHz.

### Pharmacology

Isoproterenol and isobutylmethylxanthine (IBMX) (both Sigma) were prepared in an aqueous solution containing ascorbic acid (1 mg/ml). Okadaic acid (LC Services, Woburn, MA) was dissolved in dimethylsulfoxide to form a stock solution of 1.25 mM. The stock solution was diluted in bath solutions as required; the final dimethylsulfoxide concentrations was <1%, and had no nonspecific effects in controls. Other chemicals were of the highest grade commercially available.

### Data analysis

Only patches that showed a single conductance level were analyzed. Standard single-channel analysis was performed by idealizing openings and closures according to a half-height criterion. The straightforward approach (biophysically) for investigating the slow cycling of a $Ca^{2+}$ channel between periods of availability and unavailability would be to obtain continuous records of single $Ca^{2+}$ channel activity at a fixed voltage that is sufficiently positive to activate an available channel (e.g., +20 mV). In principle, this approach avoids the complications entailed by failure to detect periods of channel unavailability that occur between activating voltage steps (i.e., point 2 in the Introduction). Moreover, traditional, continuous-time Markov analysis of open and closed duration histograms (Colquhoun and Hawkes, 1981) could be used to determine transition rates between available and unavailable gating "modes" (e.g., Hess et al., 1984). "Rapid gating" kinetics, characterizing millisecond gating behavior when the channel is available to open, would be embodied in the shorter time constants of duration histograms. Interconversion between available and unavailable modes would be captured by 10-fold slower time constants in the closed duration histograms, as well as by burst-duration histograms. The problem with the straightforward approach is that the cardiac $Ca^{2+}$ channel would undergo nearly complete voltage-dependent inactivation (Cavalie et al., 1986). Hence, closed durations would mainly reflect transitions from voltage-dependent inactivated states, rather than from phosphorylation-related unavailable states.

We are thus forced into a protocol where activating voltage steps are applied for short periods at regular intervals.[1] Given this restriction, we quantified slow cycling of a $Ca^{2+}$ channel between available and unavailable modes of gating as follows. Sweeps were categorized into those in which there were at least some openings (active sweeps), and those in which there were no openings throughout the depolarization epoch[2] (blank sweeps). An active sweep run is defined as a sequential string of active sweeps with the following two properties: 1) the string is uninterrupted by blank sweeps, and 2) a blank sweep immediately precedes and follows the first and last active sweep of the string, respectively. An active sweep run is therefore characterized by its length, in units of the number of constituent active sweeps. Experimentally observed active sweep runs could then be used to tabulate active sweep histograms, which plot the probability of an active sweep run lasting $\geq k$ sweeps as a function of $k$ (where $k$ is a positive integer). A similar definition holds for blank sweep runs and histograms. Sweep histograms were first proposed by Kawashima and Ochi (1988); they embody kinetic information about the slow transitions between available and unavailable modes of gating, much like traditional open and closed time histograms give us kinetic information about rapid, millisecond gating transitions. However, quantitative interpretation of sweep histograms presents a special challenge. The customary continuous-time Markov model (e.g., Colquhoun and Hawkes, 1977 and 1978l; Aldrich et al., 1983) cannot be used directly to interpret sweep histograms, because the traditional model requires that we observe channel availability continuously, without the gaps inherent to the experimental design. It turns out that a discrete-time Markov model provides the appropriate formalism (Luenberger, 1979): this class of model takes full account of silent transitions among gating modes that transpire in the gaps between observation periods; the discrete-time model describes how slow transitions among available and unavailable modes would appear if observations are restricted to discrete, periodically repeating instances, just as the requisite experimental design provides. We will develop a discrete-time Markov model in the Results section, thereby allowing us to obtain rigorous estimates of transition rates among available and unavailable modes of gating by comparison of model predictions and experimentally tabulated sweep histograms.

Statistical analysis was performed with one-tailed $t$ tests, using the paired format when appropriate. Results were considered significant at the level of $p < 0.05$. Averaged data are presented as mean ± S.E.

## RESULTS

Fig. 1 shows the effects of cAMP-dependent stimulation by isoproterenol and IBMX in a patch containing a single L-type $Ca^{2+}$ channel. Overall channel activity is markedly increased from control, as the comparison of specimen sweeps during control (left column) and drug exposure (right column) illustrates. The enhanced ensemble average current arises from two effects. First, even within active sweeps (marked "+"), the mean open probability is moderately increased, largely due to a decrease in closed times. Second, the availability of a channel to open on a given sweep is increased, as demonstrated by the enlarged fraction of active sweeps. The al-

[1]In fact, the design of our voltage protocol minimizes the influence of voltage-dependent inactivation: the holding potential of −100 mV is more than sufficiently hyperpolarized to render any steady-state, voltage-dependent inactivation unlikely (Cavalie et al., 1986; Ochi and Kawashima, 1990), and the depolarizing steps to +20 mV are short (150 ms) to limit the development of voltage-dependent inactivation (Yue et al., 1990a). On the other hand, it is important to note that the 150-ms duration of our voltage steps is sufficiently long to allow any channel that is available to open the opportunity to show itself (first latencies are typically far shorter than 150 ms at +20 mV (Yue et al., 1990b)). The use of $Ba^{2+}$ as the charge carrier largely eliminates the presence of $Ca^{2+}$-sensitive inactivation in these experiments (Yue et al., 1990a; Imredy and Yue, 1992).

[2]Note that with a lowpass filter cutoff of 1 kHz, a pattern of gating with very infrequent and brief openings (mode $0_a$ gating in Yue et al. (1990b)) will rarely be detected. Sweeps manifesting this sparse type of activity are therefore categorized as blank sweeps in our analysis.

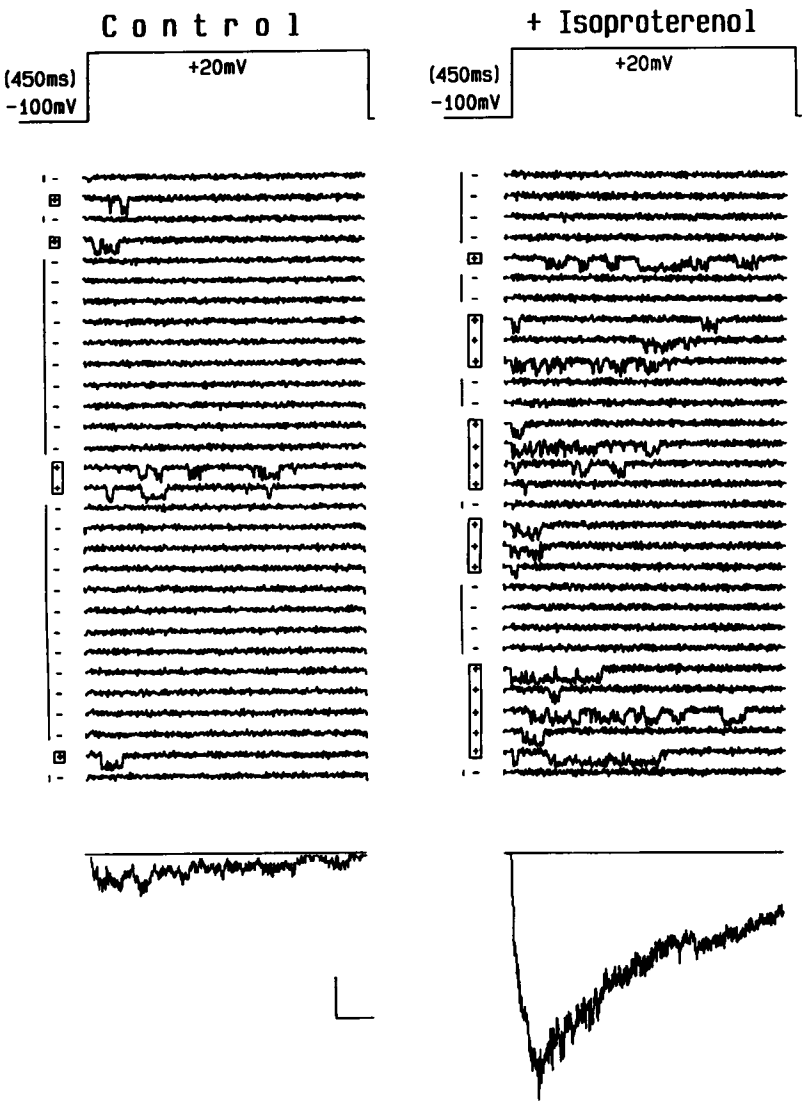


FIGURE 1 Sequential unitary current records (*top*) and ensemble averages (*bottom*) of a single L-type $Ca^{2+}$ channel before (*left*) and after (*right*) stimulation with isoproterenol (0.86 μM) and IBMX (8.6 μM). The pulse protocol is depicted on top, with voltage steps delivered every 0.6 s. Scale bars represent 2 ms and 2 pA (*top*), or 0.02 pA (*bottom*), respectively. Sweeps were labeled active ("+") or blank ("-") depending on whether they displayed openings reaching ≥ 90% of the full-conductance level. This largely prevented the identification of the so-called "mode$0_a$" activity (Yue et al., 1990b) as being active sweeps.

teration in channel availability derives from lengthening of active sweep runs (boxes around the "+" signs), and shortening of blank sweep runs (bars at left of the "–" signs). Average results of five such patches (Table 1) confirm these findings.

To understand the kinetic features underlying channel cycling among available and unavailable modes, active and blank sweep histograms were compiled from data like that in Fig. 1 (see Methods for details). Fig. 2 shows sweep histograms (*circles*) calculated from a single patch in which 480

**TABLE 1 Statistical evaluation of 10 single-channel patches**

| | Control cells | | Okadaic acid-treated cells | |
|---|---|---|---|---|
| | Baseline | Isoproterenol | Baseline | Isoproterenol |
| Slow gating | | | | |
| Active/total sweeps | 22.9 ± 4.8% | 53.3 ± 9.9% | 24.0 ± 1.9% | 38.3 ± 5.3%* |
| Active run lifetime | 1.3 ± 0.3 s | 3.4 ± 1.1 s | 1.7 ± 0.3 s | 1.7 ± 0.3 s* |
| Blank run lifetime | 5.0 ± 1.2 s | 2.2 ± 0.7 s | 4.0 ± 0.4 s | 2.5 ± 0.4 s |
| Fast gating | | | | |
| Open probability | 9.8 ± 2.5% | 17.5 ± 2.1% | 2.7 ± 0.7% | 3.2 ± 0.4% |
| Mean open time | 1.0 ± 0.0 ms | 1.1 ± 1.1 ms | 0.7 ± 0.1 ms | 0.7 ± 0.1 ms |
| Mean closed time | 4.1 ± 0.7 ms | 2.2 ± 0.2 ms | 9.6 ± 1.2 ms | 6.9 ± 1.3 ms |
| Mean first latency | 26.3 ± 3.3 ms | 15.5 ± 1.2 ms | 26.7 ± 2.9 ms | 20.8 ± 1.7 ms |

Data represents five controls, as in Fig. 1, and five pretreated with okadaic acid, as in Fig. 5.

* Denotes whether the relative effect of isoproterenol in the presence of okadaic acid was different from the isoproterenol effect in control cells (unpaired *t* test). Lifetimes expressed in units of seconds can be converted to units of sweeps by dividing by the repetition interval, 0.6 s in all cases.

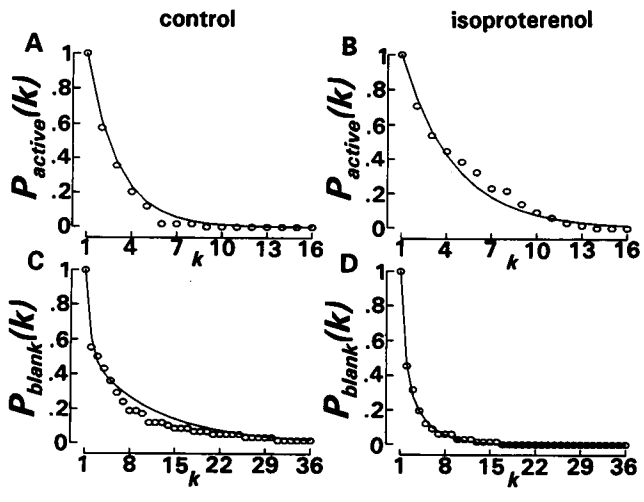


FIGURE 2 Active (*top row*) and blank (*bottom row*) sweep histograms from a single L-type $Ca^{2+}$ channel before (*left column*) and after (*right column*) stimulation with isoproterenol. The curves show fits of model Ia to data from this particular patch. Upon addition of isoproterenol, $k12$ increased from 0.18 to 0.56 $s^{-1}$, while $k21$ decreased from 0.38 to 0.23 $s^{-1}$. Small changes in $k32$ (from 3.84 to 4.00 $s^{-1}$) and $k23$ (from 1.40 to 0.85 $s^{-1}$) were not borne out statistically in averages from five patches (Fig. 4).

control sweeps and 292 isoproterenol sweeps were obtained. The solid curves have theoretical significance as discussed below. The top row shows active sweep histograms in control (*A*) and after addition of isoproterenol (*B*). The plots are well described by a single, discrete exponential function of the form (*solid curve*):

$$P_{\text{active}}(k) = \lambda_{\text{active}}^{k-1}, \tag{1}$$

where $\lambda_{\text{active}}$ ($0 \leq \lambda_{\text{active}} \leq 1$) increases with isoproterenol in a manner consistent with an increase in the mean length of active sweep runs from 2.3 to 4.0 sweeps. From discrete-time Markov theory, the presence of a single discrete exponential implies the existence of only a single mode of gating in which the channel is available to open (Luenberger, 1979). We will refer to this gating mode as "A2" (*A* for "active") and envisage that A2 contains the usual topology of closed (C) and open (O) states (C=C= · · · =C=O) used to describe rapid gating kinetics of a $Ca^{2+}$ channel (e.g., Cavalie et al., 1986). The detection of only a single active gating mode argues against the proposal that phosphorylation of any one of multiple sites can render the channel available to open (the third hypothesis in the Introduction).

The bottom row (Fig. 2) shows the corresponding blank sweep histograms for the control (C) and isoproterenol-treated (D) conditions. Both are consistent with the sum of two discrete exponential functions in the form (solid curves):

$$P_{\text{blank}}(k) = a_{\text{fast}}\lambda_{b,\text{fast}}^{k-1} + (1 - a_{\text{fast}})\,\lambda_{b,\text{slow}}^{k-1}, \tag{2}$$

where $0 \leq a_{\text{fast}} \leq 1$, $0 \leq \lambda_{b,\text{fast}} \leq 1$, $0 \leq \lambda_{b,\text{slow}} \leq 1$, and $\lambda_{b,\text{fast}}$ (corresponding to the fast-decaying component) $< \lambda_{b,\text{slow}}$. Isoproterenol decreases the average length of blank sweep runs (here from 5.9 to 2.4 sweeps), mainly by alterations of the slow component parameters. Based on discrete-time Markov theory, the biexponential form implies the existence of two modes of gating in which the channel is unavailable to open (Luenberger, 1979). We will refer to these two gating modes as B1 and B3 (B for "blank"), and presume that B1 and B3 each contain the routine topology of closed (C) and open (O) states (C=C= · · · =C=O), except that the transition from the rightmost closed state to the open state is very unlikely. Such a presumption seems required to accord with the lack of effect of isoproterenol upon cardiac $Ca^{2+}$ channel gating currents (Hadley and Lederer, 1991).

How do the three modes of gating (A2, B1, and B3) relate to phosphorylation? Since isoproterenol (or cAMP-dependent phosphorylation (Yue et al., 1990b)) increases the overall fraction of active sweeps (Table 1), A2 must be at least singly phosphorylated. Similarly, since the fraction of blank sweeps decreases with enhanced phosphorylation, at least one of the blank modes of gating must be dephosphorylated. We assign B1 to be dephosphorylated. Given these constraints, the chief possibilities for the arrangement of phosphorylations are enumerated (I through IV) in Fig. 3 *A*. To distinguish among the possibilities, we consider the fraction of active sweeps observed with very high stimulation of channel phosphorylation. The fraction of active sweeps under extremely intense stimulation never reaches 100%; in fact, the fraction seems to asymptote at a value considerably less (≈50–60% in Table 1, and in Yue et al. (1990b)). This result seems inconsistent with all the possibilities except model I. If B3 had a lower degree of phosphorylation than A2 (models II and III), the fraction of active sweeps should approach 100% with extremely high levels of kinase activity. If B3 had a higher degree of phosphorylation than A2 (model IV), the fraction of active sweeps should decline toward lower levels with high stimulation of kinase activity. Accordingly, we concentrate on variations of model I, although a further test of our choice of model I will be performed below.

Fig. 3 *B* shows the possible configurations of model I in the form of customary continuous-time Markov models, with conventional rate constants in units of reciprocal time (we have not yet made the transformation to discrete-time Markov models). Model Id can be immediately dismissed because it seems unlikely to reproduce the marked isoproterenol-induced lengthening of active sweep histograms, there being no phosphorylation-dependent transition communicating with A2. For simplicity, we first implement the discrete-time Markov equations for model Ia. If model Ia is correct, then subsequent fits of the Ia model to data will confirm that rate constants k23 and k32, which are phosphorylation independent, do not change with isoproterenol. If, on the other hand, either model Ib or Ic is true, then Ia model fits to data will show that k23 and/or k32 apparently change with isoproterenol because actual phosphorylation-dependent changes in k13 and/or k31 will be "absorbed" within the fitted values of k23 and k32. As well, fitted values of k23 and k32 should also change with isoproterenol if

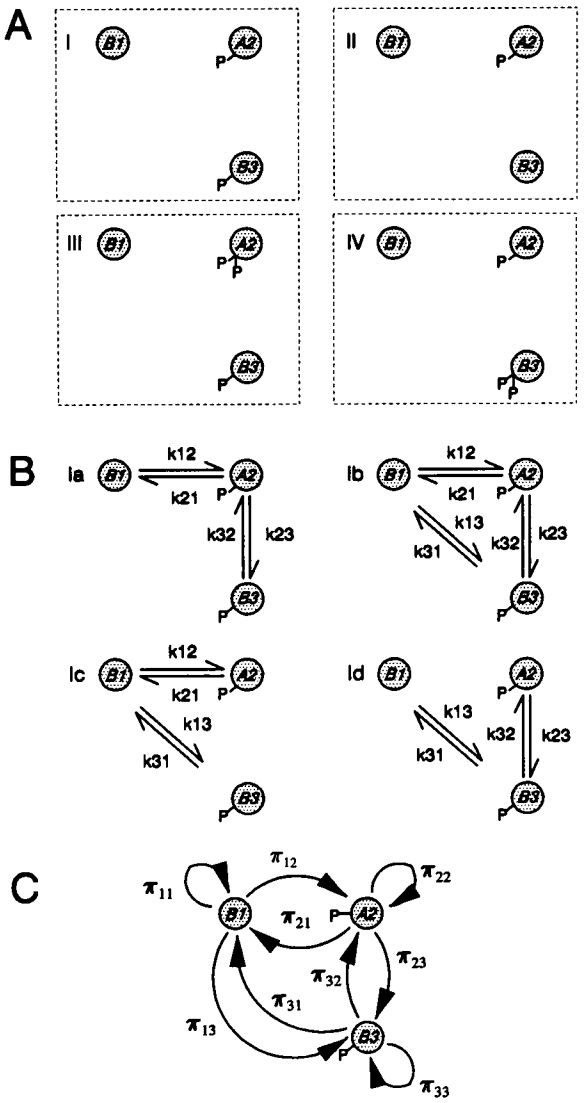


FIGURE 3 Potential topologies of active and blank modes of gating. (*A*) Possible levels of phosphorylation for the three, kinetically identified modes of gating (models I through IV). Double phosphorylations can be interpreted more generally as belonging to a class in which two or more phosphates are present. (*B*) System of continuous-time transitions that are possible for model I, denoted models Ia through Id. The diagrams correspond to continuous-time Markov representations of the models. (*C*) Discrete-time Markov representation of the continuous-time Markov processes shown in *B*.

model III, IV, or most variations of model II is true, owing to the different phosphorylation level of A2 and B3 in these schemes.

To quantitate sweep histograms, we recast the continuous-time Markov version of model Ia into an equivalent discrete-time Markov chain, as represented in Fig. 3 *C*. Each of the circles represents a possible mode in which the channel can be found every 0.6 s (during voltage steps). The arrows represent possible transitions that the channel can undergo from one step to the next. Notice that direct transitions between B1 and B2 are possible in the discrete-time model, despite the absence of such transitions in the continuous-time version of model Ia (Fig. 3 *B*). This difference arises because a channel may reside in mode B1 on one sweep and mode B2 on the next, having traversed mode A2 (perhaps multiple times) in the interim between sweeps. Although the channel must, in reality, go "through" mode A2, the channel makes an apparently direct transition from B1 to B3 when viewed within the discrete-time format. Each discrete transition is characterized by a constant transition probability $\pi_{ij}$ that describes the probability of finding the channel in mode $j$ on a specified sweep, given that the channel was in mode $i$ on the immediately preceding sweep. For example, $\pi_{12}$ is the probability of a channel being found in mode A1 on one sweep, and B2 on the next; $\pi_{11}$ is the probability of a channel being found in mode A1 on two consecutive sweeps. The fact that such transition probabilities ($\pi_{ij}$) are scalar constants (not variables) derives from the Markov assumption that the present state of a system determines all future behavior (Luenberger, 1979). Once the $\pi_{ij}$ are specified, sweep histogram behavior is entirely specified as elaborated below.

The discrete-time Markov model is completely described by a discrete-time master equation that incorporates all $\pi_{ij}$ (Luenberger, 1979). In canonical form:

$$[P_{A2}(k+1) \vdots P_{B1}(k+1)\ P_{B3}(k+1)] = [P_{A2}(k) \vdots P_{B1}(k)\ P_{B3}(k)] \begin{bmatrix} \pi_{22} & \vdots & \pi_{21} & \pi_{23} \\ \cdots & \vdots & \cdots & \cdots \\ \pi_{12} & \vdots & \pi_{11} & \pi_{13} \\ \pi_{32} & \vdots & \pi_{31} & \pi_{33} \end{bmatrix} \quad (3)$$

where $P_i(k)$ is the probability of a channel being in mode $i$ on the $k$th sweep, and all sweeps are numbered sequentially according to their temporal occurrence. Equation 3 is a subset of the general canonical form shown in Eq. 4 below. Our subsequent derivations will refer to the general equation below, because the theoretical results pertain to any discrete-time model of this form (i.e., with any number of active and blank modes).

$$\vec{P}(k+1) = [\vec{P}_A(k+1) \vdots \vec{P}_B(k+1)] = [\vec{P}_A(k) \vdots \vec{P}_{B1}(k)] \begin{bmatrix} \pi_{AA} & \vdots & \pi_{AB} \\ \cdots & \vdots & \cdots \\ \pi_{BA} & \vdots & \pi_{BB} \end{bmatrix} \quad (4)$$

where the row vectors $\vec{P}_A$ and $\vec{P}_B$ are comprised of scalar probabilities for all active or blank modes, respectively; the submatrices are defined by analogy to their specific counterparts in Eq. 3; and the entire square matrix may also be referred to in shorthand as $[\pi]$.

Once the sweep histogram problem is cast in this format, the requisite results follow from discrete-time Markov chain theory (Luenberger, 1979). Induction of Eq. 4 yields the general solution that describes the probability of a channel being in a specified mode on an arbitrary sweep $k$ ($\vec{P}(k)$, where $k$ is a positive integer $\geq 1$), given that the probabilities of

occupying a particular mode on sweep 1 is specified by the row probability vector $\vec{P}(1)$:

$$\vec{P}(k) = \vec{P}(1)[\pi]^{k-1}. \tag{5}$$

The predictions for active and blank sweep histograms take advantage of the submatrices we have defined in Eq. 4 and the theory of classes of communicating states (Luenberger, 1979). The results are

$$P_{\text{active}}(k) = [\vec{P}_{\text{A}}(1)][\pi_{\text{AA}}]^{k-1}\begin{bmatrix}1\\ \vdots \\ 1\end{bmatrix} \tag{6}$$

$$P_{\text{blank}}(k) = [\vec{P}_{\text{B}}(1)][\pi_{\text{BB}}]^{k-1}\begin{bmatrix}1\\ \vdots \\ 1\end{bmatrix} \tag{7}$$

where $\vec{P}_{\text{A}}(1)$ specifies the probabilities of finding a channel in the various active modes on sweep 1, given that the channel was in a blank mode on sweep 0; and $\vec{P}_{\text{B}}(1)$ specifies the probabilities of finding a channel in the various blank modes on sweep 1, given that the channel was in an active mode on sweep 0. Hence, if we could calculate these two probabilities, we would have explicit discrete-time Markov model predictions for active and blank sweep histograms, derivable from knowledge of the customary rate constants in Fig. 3 *B*. The derivation of these "initial probabilities" is not a standard result from discrete-time Markov theory. However, by direct analogy to the strategy for solving the comparable entity in the continuous-time case (Eq. 65 in Colquhoun and Hawkes (1977)), we can derive the requisite initial probabilities for the discrete-time case as:

$$[\vec{P}_{\text{A}}(1)] = \frac{[\vec{P}_{\text{B}}(\infty)][\pi_{\text{BA}}]}{[\vec{P}_{\text{B}}(\infty)][\pi_{BA}]\begin{bmatrix}1\\ \vdots \\ 1\end{bmatrix}} \tag{8}$$

$$[\vec{P}_{\text{B}}(1)] = \frac{[\vec{P}_{\text{A}}(\infty)][\pi_{\text{AB}}]}{[\vec{P}_{\text{A}}(\infty)][\pi_{\text{AB}}]\begin{bmatrix}1\\ \vdots \\ 1\end{bmatrix}} \tag{9}$$

where $\vec{P}_{\text{A}}(\infty)$ and $\vec{P}_{\text{B}}(\infty)$ are vectors containing the steady-state probabilities of a channel occupying the various modes. The analytic form for these can be easily calculated by the King-Altman rule (Hill, 1977). With Eqs. 6–9 in hand, we can calculate active and blank sweeps histograms given a set of traditional rate constants (Fig. 3 *B*), once the matrix $[\pi]$ is determined.

The required matrix $[\pi]$ is found by evaluation of the solution for the continuous-time master equation (Eq. 9 in Colquhoun and Hawkes (1977)),

$$\frac{d}{dt}[\vec{P}(t)] = [\vec{P}(t)][Q], \tag{10}$$

where $[Q]$ is comprised of various combinations of the contiuous-time rate constants. For example, the explicit equation for model Ia (Fig. 3 *B*) is:

$$\frac{d}{dt}[P_{\text{A2}}(t)\ P_{\text{B1}}(t)\ P_{\text{B3}}(t)] \tag{11}$$

$$= [P_{\text{A2}}(t)\ P_{\text{B1}}(t)\ P_{\text{B3}}(t)]\begin{bmatrix}-(k21 + k23) & +k21 & +k23\\ +k12 & -k12 & 0\\ +k32 & 0 & -k32\end{bmatrix}$$

The solution to this first-order, linear differential matrix equation is the matrix exponential function, which can be solved by Laplace transform techniques (Luenberger, 1979):

$$[e^{Qt}] = \mathscr{L}^{-1}\{[s[I] - [Q]]^{-1}\}. \tag{12}$$

The meaning of this matrix function is grasped by considering the element located at the $i$th row and $j$th column (Luenberger, 1979): $[e^{Qt}]_{ij}$ is the probability of finding the channel in mode $j$ at time $t$, given that the channel was in mode $i$ at time zero (also written as $P(j\ @\ t \mid i\ @\ 0)$). For example, $[e^{Qt}]$ corresponding to the specific case in Eq. 11 is given by:

$$[e^{Qt}] = \begin{bmatrix}P(\text{A2 @ } t \mid \text{A2 @ 0}) & P(\text{B1 @ } t \mid \text{A2 @ 0}) & P(\text{B3 @ } t \mid \text{A2 @ 0})\\ P(\text{A2 @ } t \mid \text{B1 @ 0}) & P(\text{B1 @ } t \mid \text{B1 @ 0}) & P(\text{B3 @ } t \mid \text{B1 @ 0})\\ P(\text{A2 @ } t \mid \text{B3 @ 0}) & P(\text{B1 @ } t \mid \text{B3 @ 0}) & P(\text{B3 @ } t \mid \text{B3 @ 0})\end{bmatrix} \tag{13}$$

Thus, it can be seen that:

$$[e^{Qt}]_{t=0.6\text{s}} = [\pi] \tag{14}$$

We now have a generalized method for transforming a continuous-time Markov model (e.g., Fig. 3 *B*) into its equivalent discrete-time Markov model (Fig. 3 *C*), in a form suitable for predicting active and blank sweep histograms. It is straightforward to derive the particular solutions for model Ia according to these general methods; they are given in the Appendix.

To estimate the rate constants that account for experimentally observed active and blank sweep histograms, a numerical routine compares model predictions for active and blank sweep histograms (from Eqs. 6–9 and 14) to actual data, and the differences between the two are minimized by varying the rate constants ($k12$, $k21$, $k23$, and $k32$) according to a gradient search algorithm (details in Appendix). The curves in Fig. 2 represent the predictions of model Ia after error minimization with respect to data from a single patch (independent estimates for the four rate constants were made for control and isoproterenol conditions). The summary of fits from five patches (Fig. 4) shows that, upon addition of isoproterenol, $k12$ increases, while $k21$ decreases. The lack of change in $k23$ and $k32$ with isoproterenol provides an important validation of the Ia mechanism. The insensitivity to isoproterenol is consistent with an identical phosphorylation state of modes A2 and B3, thereby fulfilling a key prediction of model Ia. The lack of change of these rate constants not only argues against models Ib and Ic, which propose that

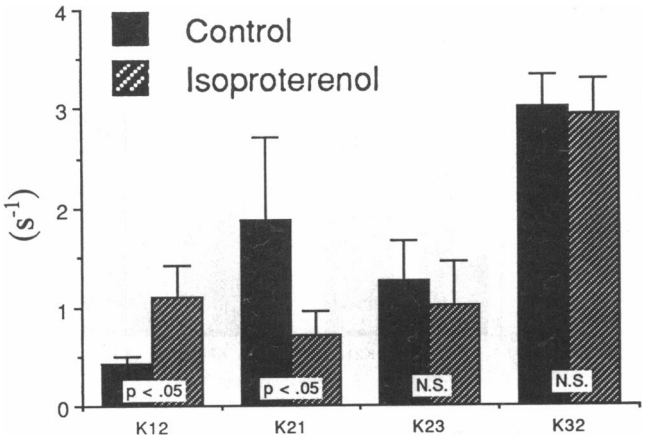


FIGURE 4 Model Ia parameters obtained during control and isoproterenol conditions. The bar graphs show mean parameter values and standard errors, derived from individual fits to five patches. Data from control and isoproterenol conditions were obtained from each patch, allowing paired *t* tests to be used in evaluating the statistical significance of changes with isoproterenol. The *t* tests were performed on the natural logarithm of rate constants, so that the underlying requirement for normally distributed random variables was satisfied. N.S. signifies no statistical significance.

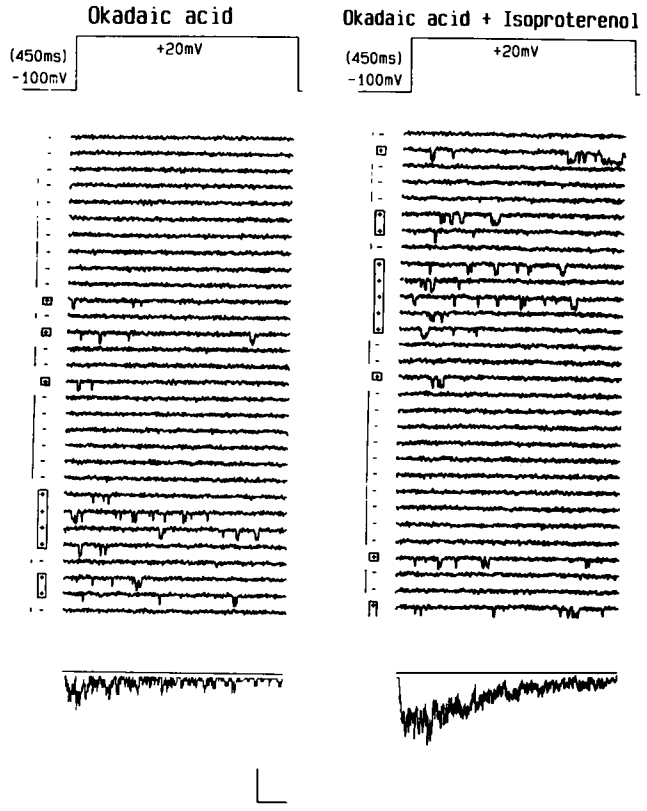


FIGURE 5 Sequential records of elementary $Ba^{2+}$ current (*top*) and their ensemble averages (*bottom*) from a single, L-type $Ca^{2+}$ channel during exposure to okadaic acid (*left column*), or to okadaic acid and isoproterenol (*right column*). The cell was initially pretreated with 6.8 μM okadaic acid for 65 min before recording 480 sweeps. Some of these are shown at left. Isoproterenol and IBMX (0.78 μM and 7.8 μM, respectively) were subsequently added, and a further 840 traces were obtained. The records at right are derived from the latter group. The pulse protocol (*top*) is identical to that in Fig. 1. (+) Active sweeps; (-) blank sweeps. Scale bars represent 20 ms and 2 pA (*top*) or 0.01 pA (*bottom*), respectively.

there are actually phosphorylation-dependent transitions between B3 and A1, but also against models II–IV, which postulate different levels of phosphorylation on A2 and B3.

To test further for the regulation of channel dephosphorylation by isoproterenol, we asked whether the protein phosphatase inhibitor, okadaic acid, affected the putative dephosphorylation rate, *k*21, and its regulation. The compound was added to the cells in concentrations of 5.9 to 12.5 μM, and cell-attached recordings were obtained 70–220 min afterwards. Under these conditions, phosphatase types 1 and 2A should be largely inhibited; only phosphatase types 2B ($Ca^{2+}$-calmodulin-dependent) and 2C should still be appreciably active (Hescheler et al., 1988). Phosphatase type 1 is particular relevant to our consideration here, having been shown to down-regulate $Ca^{2+}$ channels (Hescheler et al., 1987; Zhao et al., 1993). The control traces observed in single-channel patches were not much different from controls without such pretreatment (Fig. 5, *left panel*; and Table 1), although okadaic acid increases single-channel activity when added acutely (Neumann et al., 1993). The additional presence of isoproterenol, however, markedly altered the activity (Fig. 5, *right panel*, and Table 1). The increase in the mean open probability within active sweeps, due to changes in fast gating, was preserved; and an enhancement of the fraction of active sweeps was still clearly visible. This was now due only to the fact that the mean length of blank sweep runs was shortened (Fig. 5, bars at left of the "-" signs; Table 1). The effect of isoproterenol on the mean length of active sweep runs was absent, implicating a role of protein phosphatases in this property (Table 1).

Active and blank sweep histograms offer a more quantitative assessment of the effects of okadaic acid. Fig. 6 shows sweep histograms (*circles*) calculated from a single patch in which 480 control sweeps (with okadaic acid pretreatment) and 840 isoproterenol sweeps (ontop of okadaic acid) were obtained. The curves show the model Ia fits to the data, with separate fits of rate constants (*k*12, *k*21, *k*23, and *k*32) to the control and isoproterenol conditions. The overall numerology of exponential components is preserved from the case without okadaic acid (Fig. 2), arguing that the same Ia mechanism pertains to this case. The active sweep histograms in the top row, corresponding to control (A) and isoproterenol conditions (B), are again well described by a single discrete exponential function, consistent with a single active mode. The consistent evidence for a single, active gating mode under all four conditions provides a strong argument against the idea that phosphorylation of any one of several sites could render the channel available to open (hypothesis 3 in Introduction). With okadaic acid present constitutively, however, the active sweep histogram is essentially unchanged with isoproterenol (mean length of about 2.5 sweeps). The bottom row of blank sweep histograms, relating to control (C) and isoproterenol (D) conditions, are described

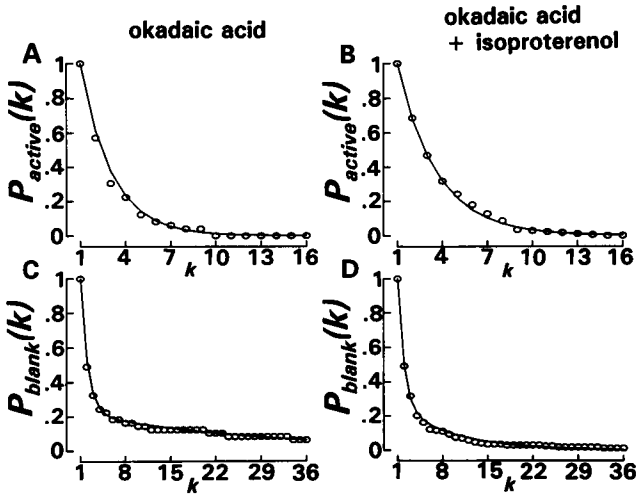


FIGURE 6 Effect of isoproterenol upon active and blank sweep histograms during phosphatase inhibition by okadaic acid. The solid curves show the model Ia fit to the data shown (*circles*), obtained from a single patch. Upon addition of isoproterenol, $k12$ increased from 0.06 to 0.21 $s^{-1}$, but had little effect upon $k21$ (from 0.15 to 0.15 $s^{-1}$), $k23$ (from 1.54 to 1.13 $s^{-1}$), and $k32$ (from 2.66 to 2.73 $s^{-1}$).

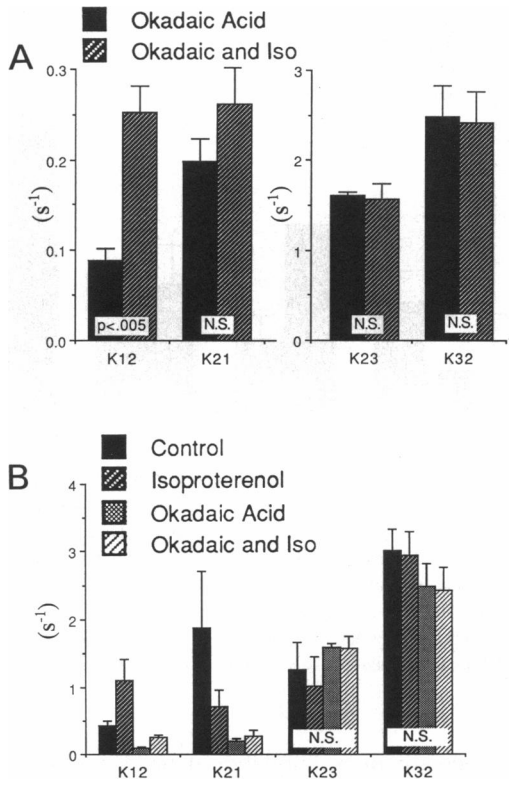


FIGURE 7 Isoproterenol-related changes in model Ia parameters, given a constant background of phosphatase inhibition by okadaic acid. (*A*) Mean and standard error for parameter estimates derived from individual fits to five patches. Each patch yielded data during periods of exposure to okadaic acid alone, as well as to okadaic acid + isoproterenol. Hence, paired *t* tests could be performed to evaluate the statistical significance of changes with isoproterenol, as detailed in the legend of Fig. 4. One patch was excluded from analysis because the blank sweep histogram became monoexponential upon addition of isoproterenol, thereby rendering it mathematically impossible to obtain model Ia parameter estimates in this instance. (*B*) Compilation of the mean and standard error of parameter estimates for all four conditions (data from *A* and Fig. 4 reproduced here). The decreases in $k12$ and $k21$ upon addition of okadaic acid (control versus okadaic acid) are significant, as is the decrease of $k12$ when okadaic acid is included ontop of isoproterenol (isoproterenol versus isoproterenol + okadaic acid). The decrease in $k21$ when okadaic acid is included in addition to isoproterenol (isoproterenol versus isoproterenol + okadaic acid) is not significant. In this panel, the unpaired format of the *t* test was used.

by a bi-discrete exponential function, consistent with two blank modes in okadaic acid as well. In contrast to the lack of effect upon active sweep histograms, isoproterenol decreases the average length of blank sweep runs (from 7.2 to 4.2 sweeps). As was observed without okadaic acid, the shortening of blank sweep histograms transpires mainly by reducing the slow component amplitude. The summary of model fits for five patches (Fig. 7 *A*) reveals that $k21$, the putative dephosphorylation rate, is indeed depressed by okadaic acid, either with or without the simultaneous presence of isoproterenol (compare control $k21$ in Figs. 4 and Fig. 7 *A*). Moreover, isoproterenol produces a striking increase in $k12$, despite the lack of appreciable change in $k23$, $k32$, and $k21$. A crucial confirmation of the Ia mechanism comes again with the lack of change of $k23$ and $k32$ with isoproterenol. In fact, $k23$ and $k32$ are unchanged with respect to any of the four conditions (control, isoproterenol, okadaic acid, okadaic acid + isoproterenol), as Fig. 7 *B* shows. We therefore interpret the increase of $k12$ with isoproterenol (Fig. 7 *A*) to reflect stimulation of PKA activity in the presence of a constant background of phosphatase inhibition by okadaic acid. The lack of change of $k21$ with isoproterenol added ontop of okadaic acid provides additional support for the down-regulation of dephosphorylation by isoproterenol under control conditions. Okadaic acid should have maximally inhibited many protein phosphatases (see above) before the addition of isoproterenol, thus ablating the ability of isoproterenol to decrease $k21$ further as a result of phosphatase inhibition.

## DISCUSSION

The main finding in this report is that there is, indeed, an intimate relationship between phosphorylation and the availability of a cardiac, L-type $Ca^{2+}$ channel to open with depolarization. In fact, our data and analysis lead us to suggest a specific proposal about how phosphorylation and availability are linked. Based upon interpretation of sweep histograms by a quantitatively appropriate formalism (i.e., discrete-time Markov model), we argue that slow cycling (> hundreds of ms) of the channel among three gating modes explains the kinetic interchange of a channel between periods of availability and unavailability. Two of the modes appear to be singly phosphorylated (A2, B3), while the other mode (B1) is likely to be dephosphorylated. Model analysis of sweep histogram data also provides evidence that β-adrenergic stimulation not only results in an increase in the phosphorylation rate governing transitions from B1 to A2, but also a striking decrease in the dephosphorylation rate for

the reverse transition. Hence, β-adrenergic stimulation appears to boost net channel phosphorylation by two, reciprocally acting mechanisms.

## Relation to previous work

Ochi and Kawashima (1990) pioneered the use of sweep histograms to investigate the effects of β-adrenergic stimulation upon slow cycling of $Ca^{2+}$ channels between periods of availability and unavailability. However, they argued for an indirect and complex relation between channel phosphorylation and availability, based upon the surprising result that isoproterenol increases the mean length of active sweep runs. The latter result initially suggests that isoproterenol decreases dephosphorylation rate, in contrast to the customary paradigm for the β-adrenergic cascade. When they examined their data more quantitatively, using continuous-time Markov models to interpret sweep histograms, essentially the same conclusion could have been drawn. However, as they were careful to point out, parameter estimates could be corrupted by silent, intermodal transitions transpiring between voltage steps (pp. 193–194 in Ochi and Kawashima (1990)). Thus, the apparent reduction in dephosphorylation rates could still have been an analytical artifact, one that actually reflects regulation of a complex model without altered phosphatase activity.

The difference between their conclusion and ours derives from two key points. First, the use of a quantitatively appropriate formalism to interpret sweep histograms makes it difficult to discount the apparent, isoproterenol-induced decrease in dephosphorylation rate as an analytical artifact. Second, the new experimental results with okadaic acid provide very strong support for the interpretation offered by our model. Inhibition of phosphatases by okadaic acid decreases the channel dephosphorylation rate, as gauged by our model fits to data. Preinhibition of phosphatases by okadaic acid prevents a further decrement of this apparent rate by isoproterenol, yet preserves the apparent increase in phosphorylation rate by the β-adrenergic stimulus. The concurrence of the anticipated biological effects of okadaic acid and those detected by our analysis, greatly strengthen our confidence in the model's interpretive power. Taken together, these two points provide strong evidence for the simple, and direct relation between channel phosphorylation and availability (model Ia).

The case is made even stronger by subsequent biochemical results that have been reported since the original Ochi and Kawashima (1990) study. Ahmad et al. (1989) demonstrated that isoproterenol increases the activity of inhibitor-1, an inhibitor of type 1 phosphatases. This finding is particularly relevant to $Ca^{2+}$ channels in heart, because a type 1 phosphatase has been shown to decrease the activity of cardiac $Ca^{2+}$ channels, presumably by channel dephosphorylation (Hescheler et al., 1987). Inhibitor-1 is only active when phosphorylated, and Neumann et al. (1991) have gone on to provide strong evidence that β-adrenergic stimulation enhances inhibitor-1 phosphorylation in heart, presumably as the consequence of PKA activation. These results thereby provide a likely biochemical scenario by which type 1 phosphatase activity can be decreased by isoproterenol.

## Proposed mechanisms of $Ca^{2+}$ channel regulation by β-adrenergic stimulation

Our model for $Ca^{2+}$ channel regulation is reminiscent of the original proposals by Sperelakis and Schneider (1976), and by Reuter and Scholz (1977) (RSSS hypothesis in Tsien et al., 1986). These early models contended that channel phosphorylation was required for opening, so that β-adrenergic stimulation worked mainly by increasing the number of functional channels (Bean et al., 1984). Since the original RSSS mechanisms have been subject to revision along several fronts, it is only natural to wonder whether our own model Ia requires refinement.

### *Phosphorylation-independent $Ca^{2+}$ current*

A number of reports have argued that $Ca^{2+}$ channel phosphorylation is not required for opening, in contrast to our model Ia, in which phosphorylation is obligatory for opening. In studies at the whole-cell level (Kameyama et al., 1986a and 1986b; Shuba et al., 1990), a small amount of $Ca^{2+}$ current was present despite internal dialysis of heart cells with solutions believed to minimize channel phosphorylation. At the single-channel level, $Ca^{2+}$ channels in bilayers can also open (with Bay K 8644 present), despite the absence of any kinases (Rosenberg et al., 1986). As well, L-type $Ca^{2+}$ channels in excised patches from cultured, embryonic cardiomyocytes do not seem to require phosphorylation to remain active (Mazzanti et al., 1991). On the other hand, native $Ca^{2+}$ channels in excised patches of adult cardiomyocytes require PKA phosphorylation to open (Ono and Fozzard, 1992). In addition, we invariably observed a monoexponential form for the active sweep histograms obtained under all four conditions, arguing for the predominance of a single active mode. Since the probability of active sweeps is increased with β-adrenergic stimulation, the lone active mode must be phosphorylated. Hence, phosphorylation seems to be obligatory for opening. How do we resolve the apparent discrepancy? One likely possibility involves the exclusion from our analysis of a sparse pattern of opening known as mode $0_a$ gating (Yue et al., 1990b). For simplicity, we have filtered our records at 1 kHz so that sweeps manifesting mode $0_a$ gating would be lumped together with blank sweeps. Since we have previously shown that the fraction of sweeps manifesting mode $0_a$ activity decreases with β-adrenergic stimulation (Yue et al., 1990b), it seems reasonable that mode $0_a$ has been lumped together here with the dephosphorylated blank mode (i.e., B1). Hence, small $Ca^{2+}$ currents carried by mode $0_a$ gating could be responsible for the residuum of dephosphorylation-resistant current measured at the whole-cell level. As well, the single-channel openings observed by

Rosenberg et al. (1986) in bilayers may reflect mode $0_a$ activity, which no longer appears sparse because of the prolongation of openings by Bay K 8644. Another possible resolution to the discrepancy is that the dephosphorylation-resistant current reflects incomplete inhibition of channel phosphorylation; this is extremely difficult to verify. Similarly, the continued opening of $Ca^{2+}$ channels in patches excised from embryonic heart cells may reflect slow diffusion of kinase activity and MgATP from the patch (Mazzanti et al., 1991). Hence, reports of phosphorylation-independent $Ca^{2+}$ current provide no clear-cut evidence against the main features of model Ia, but this question deserves further study.

### *Direct G-protein effects on $Ca^{2+}$ channels*

It has been argued that activated G-proteins ($G_s$, in particular) can directly interact with cardiac $Ca^{2+}$ channels to produce a part of the stimulatory effect of β-adrenergic stimulation (Yatani et al., 1987 and 1989; Mattera et al., 1989). On the other hand, serious challenges have been raised for the proposal (Hartzell et al., 1991), so the mechanism remains rather controversial. Our work is separate from the controversy, because we studied isoproterenol-induced stimulation in on-cell patches. This geometry isolates the $Ca^{2+}$ channels in our patches from isoproterenol added to the bath solution. Hence, it is unlikely that any direct G-protein interactions figure in the observed channel stimulation, which should result solely from diffusible second messenger effects. Nevertheless, if the direct G-protein effects on $Ca^{2+}$ channels turn out to be substantiated, it will be interesting to see how this modality of regulation interacts with phosphorylation-related mechanisms.

### *Alterations in rapid gating kinetics with β-adrenergic stimulation*

A serious challenge to the early RSSS models came with single-channel records showing that the rapid gating kinetics of active sweeps were changed with isoproterenol (Cachelin et al., 1983; Brum et al., 1984). The RSSS model predicts that isoproterenol should make available more functional channels, but with the same rapid gating kinetics. Model Ia, in its simplest form, has the same deficiency because there is only one active gating mode, and thereby no explicit provision for altered rapid gating.[3] The divergence of views can be resolved by the proposal that one phosphorylation site controls slow transitions between available and unavailable modes, and other sites regulate the fast kinetic changes that are expressed once the channel is available to open. So long as (de)phosphorylation for the site relating to channel availability transpires independently of the phosphorylation reactions governing rapid gating, the problem of resolving the kinetics of channel availability can be treated as an independent process in which all active sweeps can be lumped together, without regard for the phosphorylation level of the rapid-gating sites. In such a case, the quantitative rigor of our analysis is preserved. This proposal, in its general form, was originally made by Tsien et al. (1986), but it now takes on additional support from the recent biochemical evidence for multiple phosphorylation sites on L-type $Ca^{2+}$ channels (Flockerzi et al., 1986; O'Callahan and Hosey, 1988; De Jongh et al., 1989). In particular, backphosphorylation experiments demonstrate that the cardiac $\alpha_1$ subunit is phosphorylated by PKA in vivo near the carboxyl terminus (Yoshida et al., 1992), while the cardiac β subunit preserves the PKA consensus phosphorylation site (Peres-Reyes et al., 1992) that has been shown to be phosphorylated in the skeletal muscle β subunit (De Jongh et al., 1989; Ruth et al., 1989). Moreover, Ono and Fozzard (1993) have provided physiological data suggesting that different phosphorylation sites independently regulate different aspects of channel gating.

Fig. 8 shows the proposal explicitly, with our original model Ia scheme now expanded into several "stacked" copies corresponding to the phosphorylation status of the other sites that govern rapid gating kinetics. Phosphorylations along the "availability" axis permit the channel to open. Translation along the other phosphorylation axis, labelled "rapid gating," corresponds to changes in the nature of rapid-gating kinetics. If (de)phosphorylations along the availability and rapid-gating axes proceed as independent processes, then for the purpose of analyzing channel availability, it is possible to collapse the overall scheme along the rapid-gating axis into a single Ia model, as we have done. Interestingly, the regulation of rapid gating should transpire by way of discontinuous shifts according to the mechanism in Fig. 8, just as our recent electrophysiological work confirms (Yue et al., 1990b).

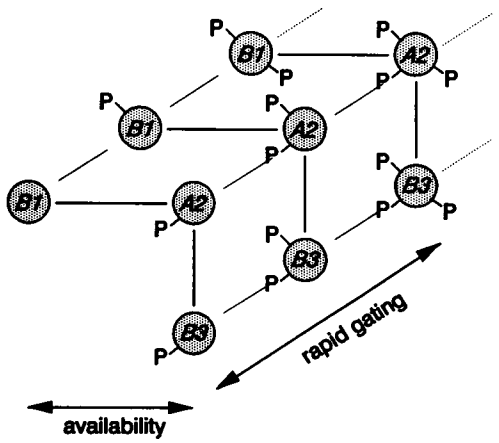


FIGURE 8 Proposed topology of $Ca^{2+}$ channel phosphorylation. The front plane contains the gating scheme investigated in this study, related to channel availability. The changes in rapid gating produced by isoproterenol suggest the existence of additional sites of modulation. This gives rise to an extension of the model involving copies of the original model which are arrayed along a perpendicular dimension.

[3]The exclusion of mode $0_a$ sweeps in our analysis would not account for the discrepancy; even when mode $0_a$ sweeps are excluded from analysis, the changes in the rapid gating of the remaining active sweeps are still profound (Yue et al., 1990b).

While the overall scheme in Fig. 8 finds support from a number of reports, the monoexponential form of our active sweep histograms serves as the only evidence for the specific requirement that (de)phosphorylations along orthogonal axes proceed independently. If the phosphorylation processes were interdependent, there should have been more than one kinetically distinguishable gating mode, as gauged by the number of exponential components in active sweep histograms. Since the specific property in question is required to preserve the quantitative rigor of our model analysis, we wanted to examine this feature of the model by an independent test. We reasoned that if the two sorts of phosphorylation interact, then the first sweep of an active sweep run might, on average, exhibit different rapid-gating kinetics than active sweeps preceded by several active sweeps. In effect, the first sweep of an active sweep run is biased toward a very short history of being phosphorylated at the availability site, while the subsequent sweeps of an active sweep run are beneficiaries of a longer history of phosphorylation at that site. If, for example, the phosphorylation that confers availability is prerequisite for phosphorylations that alter rapid gating, then the first sweep of an active run might have a particularly low degree of rapid-gating phosphorylation. On the other hand, if the two types of phosphorylation proceed independently, there should be no difference in rapid gating among the various sweeps in an active sweep run. Table 2 shows the results of the relevant tests. Active sweeps are categorized according to their position within an active run: single active sweeps were assigned to category 1, the first sweep of a longer run was put into category 2a, the last sweep into category 2b. Sweeps adjacent to at least one active sweep on each side were assigned to category 3, those with at least two neighbors on each side to category 4, and those with at least three or more neighbors to category 5. Rapid gating was then analyzed separately for the subensemble of sweeps within each of these categories, and normalized by behavior derived from the global ensemble. Three single-channel patches contained enough sweeps (>5, even within the higher categories 4 and 5) to allow for a meaningful comparison of the data acquired before and after addition of drugs (isoproterenol 0.71–1.5 μM and IBMX 7.1–15 μM). The data shows no difference in the rapid gating of sweeps as a function of their position within an active sweep run, either during control or β-adrenergic-stimulated conditions. The pronounced alterations of rapid-gating parameters with isoproterenol (e.g., mean open probability) are manifested uniformly by sweeps within the different categories. The only obvious deviation from unity is found for the first latency, which appears longer for the first two categories 1 and 2a (but not 2b). This should be expected, because of the higher probability that the transition from an unavailable to available gating mode occurs just during the voltage step (150 ms). These results provide additional evidence that the (de)phosphorylation reactions relating to channel availability proceed independently from those governing rapid gating. We thereby argue that the quantitative accuracy of our model Ia analysis is preserved within the expanded framework of Fig. 8.

## Unresolved questions

An apparently unexpected effect of okadaic acid is an overall reduction in $k12$ (Fig. 7 *B*), the presumed phosphorylation rate. On the one hand, this could be an unanticipated, nonspecific effect of okadaic acid on PKA activity, although we could not detect any such effect in vitro (not shown). A more likely explanation, however, involves the entirely anticipated interaction of okadaic acid with β-adrenergic receptor desensitization. Lefkowitz and colleagues (Hausdorff et al., 1990) have provided extensive evidence that phosphorylation of the β-adrenergic receptor by PKA and β-adrenergic receptor kinases (β-ARK) lead to receptor desensitization. Okadaic acid presumably inhibits the phosphatases responsible for antagonizing such phosphorylation-dependent desensitization, leading to an overall loss of activity of the β-adrenergic receptor, and a resultant decrease in PKA activation.

Another unusual finding is the existence of a second blank mode of gating, B2, which presumably persists in spite of phosphorylation. What is the origin of this mode? It could reflect the remnant of voltage-dependent inactivation that would persist, even at infinitely negative membrane potentials. We have tried to minimize the presence

**TABLE 2**

| | Category | | | | | |
|---|---|---|---|---|---|---|
| Gating parameter | 1 | 2a | 2b | 3 | 4 | 5 |
| Mean open time | 99.3 ± 7.2 | 97.6 ± 3.1 | 102.1 ± 3.0 | 99.1 ± 3.8 | 99.5 ± 12.8 | 97.8 ± 12.0 |
| Mean closed time | 106.9 ± 8.7 | 100.2 ± 4.2 | 110.4 ± 6.4 | 88.4 ± 2.5* | 108.2 ± 12.8 | 87.5 ± 10.9 |
| Mean first latency | 124.3 ± 17.9 | 117.2 ± 5.9* | 87.6 ± 3.5* | 101.7 ± 6.5 | 82.1 ± 4.7* | 102.5 ± 10.5 |
| Open probability | 96.4 ± 6.0 | 90.4 ± 3.4* | 97.1 ± 3.7 | 108.6 ± 5.6 | 88.5 ± 8.4 | 102.3± 10.5 |
| Number of datasets | 6 | 6 | 6 | 6 | 5 | 4 |

Values are percent of the average value found within the whole dataset (e.g., control, or isoproterenol).

Categories correspond to active sweeps surrounded by other active sweeps in ascending order (see text). The datasets are derived from three separate single-channel experiments, with $n$ = 110, 136, and 160 active sweeps studied under control conditions, and $n$ = 292, 270, and 492 active sweeps after isoproterenol addition.

* Denotes a statistically significant difference versus 100%, using an unpaired-$t$ test.

of voltage-dependent inactivation in this study by using a holding potential of −100 mV throughout. Hence, the question is open, and it will be interesting to see whether reduced holding potentials influence the transitions to and from B2 in a manner consistent with voltage-dependent inactivation.

## Molecular correlates

Our proposed mechanism of β-adrenergic stimulation (Fig. 8) stipulates that phosphorylation of different sites on a single molecular complex can proceed independently, and can regulate distinct functional behaviors. The expression of cloned cardiac L-type $Ca^{2+}$ channel subunits (Catterall, 1991), as well as the in vivo phosphorylation of the cardiac $\alpha_1$ subunit (Yoshida et al., 1992), have now been demonstrated. Hence, the tools are now at hand to test the above-mentioned postulates at the molecular level. Klöckner et al. (1992) have suggested that the β subunit appears to be necessary to confer a large degree of cAMP-dependent regulation to the overall $Ca^{2+}$ channel complex. Possibly, the effect transpires by way of PKA phosphorylation of the β subunit itself, as the biochemical evidence suggests (De Jongh et al., 1989; Ruth et al., 1989; Peres-Reyez et al., 1992). On the other hand, phosphorylation of the main $\alpha_1$ subunit seems to play at least some role in cAMP-dependent channel regulation (Flockerzi et al., 1986; Yoshida et al., 1992). It is only natural to wonder whether two phosphorylation sites correspond to our proposed "availability" and "rapid-gating" sites. Site-directed mutagenesis can be used to selectively neutralize either or both sites. If the predictions of our mechanism are correct, it should be possible to express channels whose stimulation by PKA manifests as an exclusive change in rapid gating, or as an exclusive change in channel availability. A positive result along these lines would provide a striking extension of the case for modularity in the structure-function relations of ion channel proteins.

We gratefully acknowledge Karen McCumber for assistance with data analysis and secretarial support, as well as Anne Bölle and Britta Piepenburg for technical assistance. This work was supported by Deutsche Forschungsgemeinschaft (He 1578 3-1 to S. Herzig), the National Institutes of Health (GM07309, MSTP scholarship to P. G. Patil; R29 HL43307 FIRST award to D. T. Yue), and the American Heart Association (Established Investigatorship to D. T. Yue).

## APPENDIX

Here we explicitly elaborate the discrete-time Markov model equations for model Ia. With reference to Eqs. 1 and 6, the active sweep histogram is given by:

$$P_{active}(k) = P_{A2}(1)[\pi_{22}]^{k-1} \tag{A1}$$

Similarly, the blank sweep histogram is given by:

$$P_{blank}(k) = [P_{B1}(1)\ P_{B3}(1)]\begin{bmatrix}\pi_{11} & \pi_{13}\\ \pi_{31} & \pi_{33}\end{bmatrix}^{k-1}\begin{bmatrix}1\\1\end{bmatrix} \tag{A2}$$

The initial probabilities are given by:

$$P_{A2}(1) = 1 \tag{A3a}$$

$$[P_{B1}(1)\ P_{B3}(1)] = \frac{[\pi_{21}\ \pi_{23}]}{\pi_{21} + \pi_{23}} \tag{A3b}$$

The matrix $[\pi]$ is given by the following formulae, which can be calculated on a computer. In this case, the matrix $[Q]$ is:

$$[Q] = \begin{bmatrix}q11 & q12 & q13\\ q21 & q22 & q23\\ q31 & q32 & q33\end{bmatrix} = \begin{bmatrix}-(k21 + k23) & +k21 & +k23\\ +k12 & -k12 & 0\\ +k32 & 0 & -k32\end{bmatrix} \tag{A4}$$

Next, we need to calculate $[\pi] = [e^{Qt}]_{t = 0.6\ s}$. To do so, we must take the inverse Laplace transform of $[sI - Q]^{-1}$ (after Eq. 12), where $[sI - Q]^{-1}$ is

$$\frac{\begin{bmatrix}s^2 + (-q22 - q33)s + (q22q33) & (q12)s + (-q12q33) & (q13)s + (-q13q22)\\ (q21)s + (-q21q33) & s^2 + (-q11 - q33)s + (q11q33 - q13q31) & (q13q21)\\ (q31)s + (-q31q22) & (q12q31) & s^2 + (-q11 - q22)s + (q11q22 - q12q21)\end{bmatrix}}{s(s - \lambda_1)(s - \lambda_2)} \tag{A5}$$

and

$$\lambda_1 = \frac{(q11 + q22 + q33) + [(q11 + q22 + q33)^2 - 4(q11q22 + q11q33 + q22q33 - q12q21 - q13q31)]^{0.5}}{2}$$

$$\lambda_2 = \frac{(q11 + q22 + q33) - [(q11 + q22 + q33)^2 - 4(q11q22 + q11q33 + q22q33 - q12q21 - q13q31)]^{0.5}}{2} \tag{A6}$$

For ease of computing, let's define the variables *aij*, *bij*, and *cij*, such that Eq. A5 can be rewritten:

$$\frac{\begin{bmatrix}(a11)s^2 + (b11)s + (c11) & (a12)s^2 + (b12)s + (c12) & (a13)s^2 + (b13)s + (c13)\\ (a21)s^2 + (b21)s + (c21) & (a22)s^2 + (b22)s + (c22) & (a23)s^2 + (b23)s + (c23)\\ (a31)s^2 + (b31)s + (c31) & \vdots & \vdots\end{bmatrix}}{s(s - \lambda_1)(s - \lambda_2)} \tag{A7}$$

Partial-fraction expansion of the terms in Eq. A7, and standard inverse Laplace transform tables yield the following expression for $[e^{Qt}]$. The element in the *i*th row and *j*th column of $[e^{Qt}]$ is given by:

$$[e^{Qt}]_{ij} = \left[\frac{aij\lambda_1^2 + bij\lambda_1 + cij}{\lambda_1(\lambda_1 - \lambda_2)}e^{\lambda_1 t} - \frac{aij\lambda_2^2 + bij\lambda_2 + cij}{\lambda_2(\lambda_1 - \lambda_2)}e^{\lambda_2 t} + \frac{cij}{\lambda_1\lambda_2}\right] \tag{A8}$$

where *aij*, *bij*, and *cij* are defined in Eq. A7. This can easily be evaluated for $t = 0.6$ s, yielding $[\pi]$.

The probability density form of active and blank sweep histograms ($p_{active}(k)$ and $p_{blank}(k)$, respectively) were compared with the probability density predictions (from Eqs. A1 and A2) of the model (defined here as $p_{active,\ model}(k)$, $p_{blank,\ model}(k)$). Cumulative distributions (e.g., Fig. 2), although simpler

to conceptualize, suffer from the statistical standpoint in that successive bins are correlated. This makes the cumulative distribution less suited for parameter estimation according to the least-squares algorithm described below. Accordingly, probability density functions were used to generate an error function $E$ defined as:

$$E = \left( \sum_{k \in \text{data}} [p_{\text{active}}(k) - p_{\text{active, model}}(k)]^2 + [p_{\text{blank}}(k) - p_{\text{blank, model}}(k)]^2 \right) + (F_{\text{active}} - F_{\text{active, model}})^2, \quad \text{(A9)}$$

where $k$ was indexed over all run lengths observed in either active or blank sweeps runs, $F_{\text{active}}$ is the observed fraction of active sweeps, and $F_{\text{active, model}}$ is the model Ia prediction for the overall fraction of active sweeps. From the King-Altman rule (Hill, 1977), we can calculate:

$$F_{\text{active, model}} = \frac{k12k32}{k12k32 + k21k32 + k12k23}. \quad \text{(A10)}$$

The gradient of $E$ was numerically calculated with respect to $k12$, $k21$, $k23$, $k32$, and parameters were slowly changed from initial guesses according to a steepest decent algorithm, with some initial annealing. More than 1000 iterations were used for each fit, by which time the gradient of $E$ was essentially zero (i.e., a minimum error had been found). The numerical routines and data display were implemented on a 80386-based computer with a 80387 numerical coprocessor, using programs written with AXOBASIC 1.1 software (Axon Instruments, Foster City, CA).

## REFERENCES


Ahmad, Z., F. J. Green, H. S. Subuhi, and A. M. Watanabe. 1989. Autonomic regulation of type 1 protein phosphatase in cardiac muscle. *J. Biol. Chem.* 264:3859–3863.

Aldrich, R. W., D. P. Corey, and C. F. Stevens. 1983. A reinterpretation of mammalian sodium channel gating based on single channel recording. *Nature (Lond.).* 306:436–441.

Bean, B. P., M. C. Nowycky, and R. W. Tsien. 1984. β-Adrenergic modulation of calcium channels in frog ventricular heart cells. *Nature (Lond.).* 307:371–375.

Brum, G., W. Osterrieder, and W. Trautwein. 1984. β-Adrenergic increase in the calcium conductance of cardiac myocytes studied with the patch clamp. *Pflügers Arch.* 401:111–118.

Cachelin, A. B., J. E. de Peyer, S. Kokubun, and H. Reuter. 1983. $Ca^{2+}$ channel modulation by 8-bromocyclic AMP in cultured heart cells. *Nature (Lond.).* 304:462–464.

Catterall, W. A. 1991. Functional subunit structure of voltage-gated calcium channels. *Science (Wash. DC).* 253:1499–1500.

Cavalie, A., D. S. Pelzer, and W. Trautwein. 1986. Fast and slow gating behaviour of single calcium channels in cardiac cells. Relation to activation and inactivation of calcium-channel current. *Pflügers Arch.* 406: 241–258.

Cohen, P., C. F. B. Holmes, and Y. Tsukitani. 1990. Okadaic acid: a new probe for the study of cellular regulation. *Trends Biochem. Sci.* 15:98–102.

Colquhoun, D., and A. G. Hawkes. 1977. Relaxation and fluctuations of membrane currents that flow through drug-operated channels. *Proc. R. Soc. Lond. B.* 199:231–262.

Colquhoun, D., and A. G. Hawkes. 1981. On the stochastic properties of single ion channels. *Proc. R. Soc. Lond. B.* 211:205–235.

Colquhoun, D., and A. G. Hawkes. 1983. The principles of the stochastic interpretation of ion-channel mechanisms. *In* Single-Channel Recording. B. Sakmann and E. Neher, editors. Plenum, New York. 135–175.

De Jongh, K. S., D. K. Merrick, and W. A. Catterall. 1989. Subunits of purified calcium channels: a 212-kDa form of $\alpha_1$ and partial amino acid sequence of a phosphorylation site of an independent β subunit. *Proc. Natl. Acad. Sci. USA.* 86:8585–8589.

Flockerzi, V., H. J. Oeken, F. Hofmann, D. Pelzer, A. Cavalie, and W. Trautwein. 1986. Purified dihydropyridine-binding site from skeletal muscle t-tubules is a functional calcium channel. *Nature (Lond.).* 323:66–68.

Hadley, R. W., and W. J. Lederer. 1991. $Ca^{2+}$ and voltage inactivate $Ca^{2+}$ channels in guinea-pig ventricular myocytes through independent mechanisms. *J. Physiol. (Lond.).* 444:257–268.

Hartzell, H. C., P. F. Mery, R. Fischmeister, and G. Szabo. 1991. Sympathetic regulation of cardiac calcium current is due exclusively to cAMP-dependent phosphorylation. *Nature (Lond.).* 351:573–576.

Hausdorff, W. P., M. G. Caron, and R. J. Lefkowitz. 1990. Turning off the signal: desensitization of β-adrenergic receptor function. *FASEB J.* 4:2881–2889.

Herzig, S., and J. Neumann. 1992. Role of protein phosphatases in β-adrenergic stimulation of single cardiac $Ca^{2+}$ channels. *Biophys. J.* 61:A393*a*. (Abstr.)

Hescheler, J., M. Kameyama, W. Trautwein, G. Mieskes, and H. D. Söling. 1987. Regulation of the cardiac calcium channel by protein phosphatases. *Eur. J. Biochem.* 165:261–266.

Hescheler, J., G. Mieskes, J. C. Rüegg, AS. Takai, and W. Trautwein. 1988. Effects of a protein phosphatase inhibitor, okadaic acid, on membrane currents of isolated guinea-pig cardiac myocytes. *Pflügers Arch.* 412: 248–252.

Hess, P., J. B. Lansman, and R. W. Tsien. 1984. Different modes of Ca channel gating behaviour favoured by dihydropyridine Ca agonists and antagonists. *Nature (Lond.).* 311:538–544.

Hill, T. L. 1977. Free energy transduction in biology: the steady-state kinetic and thermodynamic formalism. John Wiley and Sons, Inc., New York. 1–31.

Imredy, J. P., and D. T. Yue. 1992. Submicroscopic $Ca^{2+}$ diffusion mediates inhibitory coupling between individual $Ca^{2+}$ channels. *Neuron* 9:197–207.

Kawashima, Y., and R. Ochi. 1988. Voltage-dependent decrease in the availability of single calcium channels by nitrendipine in guinea-pig ventricular cells. *J. Physiol. (Lond.)* 402:219–235.

Kameyama, M., J. Hescheler, F. Hoffmann, and W. Trautwein. 1986a. Modulation of Ca current during phosphorylation cycle in the guinea pig heart. *Pflügers Arch.* 407:123–128.

Kameyama, M., J. Hescheler, G. Mieskes, and W. Trautwein. 1986b. The protein specific phosphatase I antagonizes the β-adrenergic increase of the cardiac Ca current. *Pflügers Arch.* 407:461–463.

Klöckner, U., K. Itagaki, I. Bodi, and A. Schwartz. 1992. β-Subunit expression is required for cAMP-dependent increase of cloned cardiac and vascular calcium channel currents. *Pflügers Arch.* 420:413–415.

Luenberger, D. G. 1979. Introduction to dynamic systems: theory, models, and applications. John Wiley and Sons, Inc., New York. 188–315.

Mattera, R., M. P. Graziano, A. Yatani, Z. Zhou, R. Graf, J. Codina, L. Birnbaumer, A. G. Gilman, and A. M. Brown. 1989. Splice variants of the α subunit of the G protein $G_s$ activate both adenylyl cyclase and calcium channels. *Science (Wash. DC).* 243:804–807.

Mazzanti, M., L. J. DeFelice, and Y.-M Liu. 1991. Gating of L-type $Ca^{2+}$ channels in embryonic chick ventricle cells: Dependence on voltage, current, and channel density. *J. Physiol. (Lond.).* 443:307–334.

Mitra, R., and M. Morad. 1985. A uniform enzymatic method for dissociation of myocytes from hearts and stomachs of vertebrates. *Am. J. Physiol.* 249:H1056-H1060.

Neumann, J., P. Boknik, S. Herzig, W. Schmitz, H. Scholz, R. C. Gupta, and A. M. Watanabe. 1993. Evidence for physiological functions of protein phosphatases in the heart. Evaluation with okadaic acid. *Am. J. Physiol.* 265:H257–H266.

Neumann, J., R. C. Gupta, W. Schmitz, H. Scholz, A. C. Nairn, and A. M. Watanabe. 1991. Evidence for isoproterenol-induced phosphorylation of phosphatase inhibitor-1 in the intact heart. *Circ. Res.* 69:1450–1457.

O'Callahan, C. M., and M. M. Hosey. 1988. Multiple phosphorylation sites in the 165 kilodalton peptide associated with dihydropyridine-sensitive Ca channels. *Biochemistry.* 27:6071–6077.

Ochi, R., and Y. Kawashima. 1990. Modulation of slow gating process of calcium channels by isoprenaline in guinea-pig ventricular cells. *J. Physiol. (Lond.).* 424:187–204.

Ono, K., and H. A. Fozzard. 1992. Phosphorylation restores activity of L-type $Ca^{2+}$ channels after rundown in inside-out patches from rabbit cardiac cells. *J. Physiol. (Lond.).* 454:673–688.

Ono, K., and H. A. Fozzard. 1993. Two phosphatase sites on the Ca channel affecting different kinetic functions. *J. Physiol. (Lond.)*. In press.

Patil, P. G., S. W. Herzig, and D. T. Yue. 1993. A new approach to modeling β-adrenergic regulation of cardiac L-type Ca channels implicates both phosphatase and kinase involvement. *Biophys. J.* 64:A344*a*. (Abstr.)

Peres-Reyes, E., A. Castellano, H. S. Kim, P. Bertrand, E. Baggstrom, A. E. Lacerda, X. Wei, and L. Birnbaumer. 1992. Cloning and expression of a cardiac/brain β subunit of the L-type Ca channel. *J. Biol. Chem.* 267: 1792–1797.

Reuter, H., and H. Scholz. 1977. The regulation of the Ca conductance of cardiac muscle by adrenaline. *J. Physiol. (Lond.)*. 264:49–62.

Rosenberg, R. I., P. Hess, R. W. Tsien, J. P. Reeves, and H. Smilowitz. 1986. Cardiac calcium channels in planar bilayers: Insights into mechanisms of ion permeation and gating. *Science (Wash. DC)*. 231:1564–1566.

Ruth, P., A. Röhrkasten, M. Biel, E. Bosse, S. Regulla, H. E. Meyer, V. Flockerzi, and F. Hoffman. 1989. Primary structure of the β subunit of the DHP-sensitive calcium channel from skeletal muscle. *Science (Wash. DC)*. 245:1115–1118.

Shuba, Y. M., H. Bernd, W. Trautwein, T. McDonald, and D. Pelzer. 1990. Whole-cell calcium current in guinea-pig ventricular myocytes dialysed with guanine nucleotides. *J. Physiol. (Lond.)*. 424:205–228.

Sperelakis, N., and J. Schneider. 1976. A metabolic control mechanism for calcium ion influx that may protect the ventricular myocardial cell. *Am. J. Cardiol.* 37:1079–1085.

Tsien, R. W., B. P. Bean, P. Hess, J. B. Lansman, B. Nilius, and M. C. Nowycky. 1986. Mechanism of calcium channel modulation by β-adrenergic agents and dihydropyridine calcium agonists. *J. Mol. Cell. Cardiol.* 18:691–710.

Yatani, A., and A. M. Brown. 1989. Rapid β-adrenergic modulation of cardiac calcium channel currents by a fast G protein pathway. *Science (Wash. DC)*. 245:71–74.

Yatani, A., J. Codina, Y. Imoto, J. P. Reeves, L. Birnbaumer, and A. M. Brown. 1987. A G protein directly regulates mammalian cardiac calcium channels. *Science (Wash. DC)*. 238:1288–1292.

Yoshida, A., M. Takahashi, S. Nishimura, H. Takeshima, and S. Kokubun. 1992. Cyclic AMP-dependent phosphorylation and regulation of the cardiac dihydropyridine-sensitive Ca channel. *FEBS Lett.* 309:343–349.

Yue, D. T., P. H. Backx, and J. P. Imredy. 1990a. Calcium-sensitive inactivation in the gating of single calcium channels. *Science (Wash. DC)*. 250:1735–1738.

Yue, D. T., S. Herzig, and E. Marban. 1990b. β-Adrenergic stimulation of calcium channels occurs by potentiation of high-activity gating modes. *Proc. Natl. Acad. Sci. USA*. 87:753–757.

Zhao, X. I., C. F. Chang, L. M. Gutierrez, and M. M. Hosey. 1993. Regulation of the dihydropyridine-sensitive calcium channels in skeletal muscle by the catalytic subunit of protein phosphatase type 1. *Biophys. J.* 64:A390*a*. (Abstr.)